LETTER

Dye−Polyelectrolyte Layer-by-Layer Self-Assembled Materials: Molecular Aggregation, Structural Stability, and Singlet Oxygen Photogeneration

Martín Mirenda,[†] Cristian A. Strassert,[‡] Lelia E. Dicelio,[†] and Enrique San Román*,[†]

INQUIMAE/DQIAyQF, Facultad de Ciencias Exactas y Naturales, University of Buenos Aires, Ciudad Universitaria, Pab. II, C1428EHA, Argentina, and CeNTech, Physikalisches Institut Westfälische Wilhelms-Universität Münster, Heisenbergstrasse 11, D-48149, Germany

ABSTRACT The interaction of rose Bengal (RB) and fluorescein (FL) with poly[diallyldimethylammonium] chloride (PDDA) was studied in layer-by-layer self-assembled thin films and in solution. The spectroscopic behavior is explained in terms of dye−dye, dye−polyelectrolyte, and in solution, dye−solvent interactions. A correlation among dye hydrophobicity, aggregation tendency, polymer folding in solution, and the stability of self-assembled films is obtained. In spite of the very high dye concentration (~1 M), RB-PDDA multilayer thin films are able to photogenerate singlet molecular oxygen, as demonstrated by chemical monitoring and IR phosphorescence detection.

KEYWORDS: layer-by-layer self-assembly • rose bengal • fluorescein • fluorescence • singlet molecular oxygen

INTRODUCTION

The inclusion of organic dyes into polymeric films and other structured media is of great interest in the development of new materials with potential applications in many areas of technology as diverse as light harvesting (1), singlet molecular oxygen ($^1O_2$) photosensitization (2), and even heterogeneous photocatalysis (3). In particular, immobilized singlet oxygen photosensitizers are found to be highly sought-after materials for practical applications, such as water decontamination, chemical reactions, and fine-chemical synthesis, because of their convenient removal from the reaction medium (4). One of the main obstacles in the development of this class of materials is the formation of molecular aggregates or statistical energy traps at the required high local concentrations, particularly if dye molecules are distributed at random (5). Nonradiative deactivation pathways are favored in this case, with the concomitant lowering of relevant photoprocess quantum yields. A long time ago, Neckers and others showed that the $^1O_2$ photogeneration quantum yield, Φ_Δ, diminishes with concentration in polystyrene-based materials, when the dye molecules are randomly distributed (6). In coincidence with these observations, San Román and co-workers reported recently that fluorescence self-quenching of Rhodamine 6G randomly adsorbed on microcrystalline cellulose sets in at loadings as low as 0.005 molecules/nm^2, with up to 50% quenching at surface concentrations in the order of 0.05 molecules/nm^2 (7). It is clear that to limit statistical energy trapping, we need architectures with a high degree of structural control at the molecular level.

An interesting strategy for the design of thin films with high dye concentrations and restricted molecule proximity is the layer-by-layer, supramolecular electrostatic self-assembly. This technique was employed originally for the alternating adsorption of colloidal particles on solid substrates (8) and extended more than 20 years later to the assembly of oppositely charged polyelectrolytes (9) and diverse soluble polyions such as nucleic acids (10) or enzymes (11) and small molecules, including dyes (12−14). A rather limited number of authors have so far related the spectroscopic properties of dyes with their degree of aggregation within films (15, 16), and in general, no reference is made to the influence of interactions among dye molecules on the stability and photoactivity of this kind of self-assembled materials. The quantitative investigation of dye aggregation is not straightforward in this case and cannot be carried out directly because the concentration of the dye, which is actually a structural part of the film, cannot be varied at will as it will be discussed later. Therefore, it is necessary to make use of indirect methods. In this context, we have recently shown that the photophysical analysis of the interaction of dye and polyelectrolyte in solution provides helpful information for the physicochemical characterization of self-assembled thin films (17).

We report now a comparative photophysical and photochemical investigation of layer-by-layer self-assembled arrays of poly[diallyldimethylammonium] chloride (PDDA) with two model xanthene dyes, rose Bengal (RB) and

* Corresponding author. E-mail: esr@qi.fcen.uba.ar.
Received for review March 8, 2010 and accepted May 19, 2010
[†] University of Buenos Aires.
[‡] Physikalisches Institut Westfälische Wilhelms-Universität Münster.
DOI: 10.1021/am100195v

Published on Web 05/24/2010

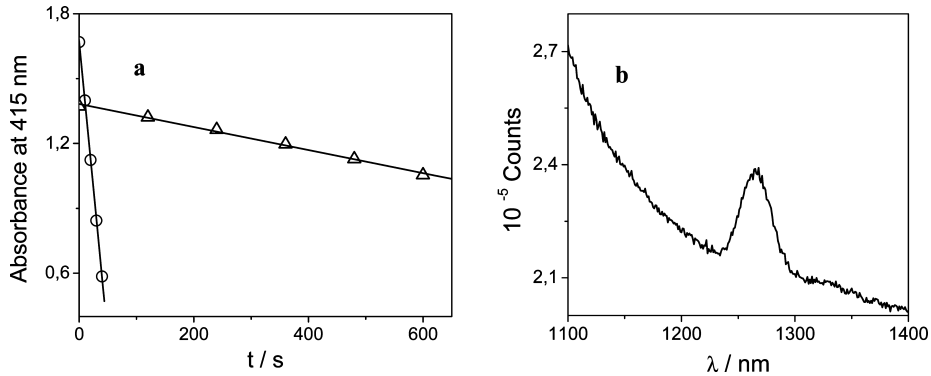

FIGURE 1. (a) DPBF absorbance decrease with increasing irradiation times employing self-assembled arrays with RB (triangles) and MB in solution (circles). (b) Steady-state phosphorescence spectrum of a self-assembled RB-PDDA array in air (λ_{ex} = 575 nm).

fluorescein (FL), as balancing counterions. The substitution pattern of the xanthene ring determines the contrasting behavior of both dyes in regard to their photophysics and aggregation tendency. On one hand, the highly hydrophilic FL evidences in solution a pH dependent fluorescence quantum yield, Φ_F, near unity in alkaline solutions (18). Quite oppositely, the rather hydrophobic RB displays a low Φ_F and a high triplet state quantum yield, Φ_T, as well as a large Φ_Δ (19). The main goal of this work is to correlate the stability and photophysical properties of the self-assembled thin films with the hydrophobicity and the aggregation tendency of the dyes. It is shown that solution experiments provide a rationale for the analysis of speciation of self-assembled materials. The photogeneration of $^1O_2$ from RB thin films is reported and discussed in terms of the film structure.

Self-Assembled Arrays of RB and PDDA. The layer-by-layer self-assembly of films on glass substrates employing RB and PDDA has been recently reported. Such arrays constitute a novel class of nanostructured materials due to their singular architectures and photophysical properties (17). The spectroscopic analysis revealed high local dye concentrations (~1 M) with a polyelectrolyte/dye ratio P/D ≈ 7, expressed in terms of dye and polyelectrolyte monomeric units. The aggregation degree is only 55%, an unusually low value for such a high chromophore density compared with the same system in solution (see Experiments in Solution below). The availability of monomeric RB suggests that irradiation of these films might lead to triplet state formation and, in the presence of dioxygen, to the photogeneration of $^1O_2$. Two independent techniques were used in order to verify this hypothesis: the bleaching of a chemical monitor that reacts with photoproduced $^1O_2$, and the stationary detection of $^1O_2$ phosphorescence at 1270 nm.

Preliminary attempts to monitor $^1O_2$ in water using *N*,*N*-dimethyl-*p*-nitrosoaniline and imidazole produced very fast desorption of RB. Therefore, 1,3-diphenylisobenzofuran (DPBF) in dichloromethane solution was used as the chemical monitor. The absorbance of the chemical monitor (λ_{max} = 415 nm) decreases noticeably when the assembled film is immersed in the solution and irradiated at the RB absorption band due to the peroxidation of DPBF by the photogenerated $^1O_2$. No decrease in the monitor absorbance is detected in the dark or under irradiation in the absence of the film.

We quantitatively tested the photosensitization quantum yield of arrays consisting of 12 bilayers of RB/PDDA at each side of the glass substrate, using a methylene blue solution (MB) as a reference ($\Phi_\Delta{}^R = 0.57$ in dichloromethane) (20). The time-dependent absorbance decrease of DPBF, obtained by irradiation of RB assemblies and MB in solution, is shown in Figure 1a. Assuming that the product of the quenching rate constant of $^1O_2$ by the concentration of DPBF is significantly higher than the decay rate constant (see the Supporting Information), it is possible to calculate Φ_Δ according to the following equation (21)

$$\Phi_\Delta = \Phi_\Delta^R \frac{I_A^R r}{I_A r^R} \quad (1)$$

where I_A stands for the absorbed photonic flux (μEinstein dm^{-3} s^{-1}) and r for the reaction rate (μM s^{-1}); superscript R identifies the reference. Results lead to $\Phi_\Delta = 0.020 \pm 0.005$. This value is much lower than the reported ones for the monomeric dye in various solvents (22), but remarkably large when taking into account the very high local concentration of the dye within the film. As the bilayer height can be estimated as 1 nm (17), photogenerated $^1O_2$ will be able to diffuse freely and react with adsorbed substrates without substantial loss within the support.

The photogeneration of $^1O_2$ was further verified by steady state infrared emission spectroscopy. Figure 1b depicts the stationary phosphorescence spectrum of a self-assembled array with 9 bilayers, measured in air upon excitation at 45°. The emission band centered at 1270 nm can be unambiguously assigned to the phosphorescence of $^1O_2$ (the growth of the baseline at the shorter wavelengths is mainly originated by light scattering). Phosphorescence is not detected if the array is previously immersed into a DPBF solution and dried, pointing to monitor adsorption. However, adsorption takes place at the trace level because it remains undetectable by absorption spectroscopy (see the Supporting Information).

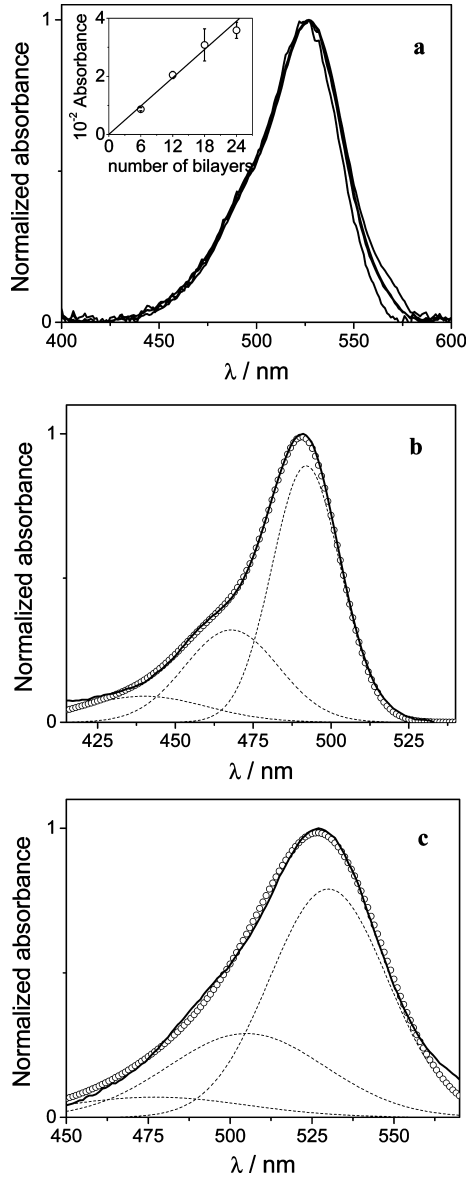

FIGURE 2. (a) Normalized average absorption spectra of self-assembled arrays with 6, 12, 18, and 24 FL/PDDA bilayers. Inset: Absorbance at the maximum as a function of the number of bilayers. The error bars represent the absorbances at different positions on the same sample, and the solid line corresponds to the linear regression through the origin of coordinates. (b) Normalized spectrum of FL in aqueous alkaline solution (solid line) and fitted (circles) by linear combination of Gaussian functions (dotted lines). (c) Normalized spectrum of a self-assembled array with FL (solid line) and fitted (circles) by linear combination of the same Gaussian functions as in b, 37 nm red-shifted and 35% widened (dotted lines).

Self-Assembled Arrays of FL and PDDA. Figure 2a depicts the normalized absorption spectra of self-assembled arrays with 3, 6, 9, and 12 bilayers of FL/PDDA at each side of the glass substrate. All spectra display the same shape, showing a maximum at 526 nm, 36 nm red-shifted with respect to aqueous alkaline solutions. Spectra in water and in the films can be decomposed as a linear combination of three Gaussians (see Figure 2b,c): each Gaussian belonging to the film can be obtained from the corresponding one in water, 37 nm red-shifted and 35% widened. This analysis suggests the sole presence of the dianionic, monomeric dye

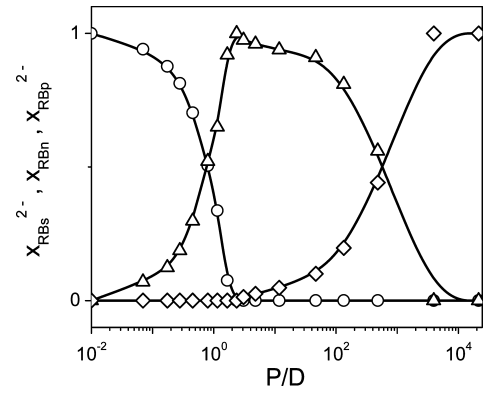

FIGURE 3. Speciation diagram of RB in PDDA solution as a function of the P/D ratio: monomer in solution (RB_S^{2-}, circles), aggregates (RB_n, triangles), and polyelectrolyte-associated monomers (RB_p^{2-}, rhomboids).

within the film. Furthermore, a markedly different ratio of bands would be observed if aggregated forms were present (23, 24). The red shift can be attributed to the increase of polarity originated by the polycationic nature of the polymeric matrix (13) and the spectral widening to heterogeneities of the microenvironment within the assembly.

These results allowed us to estimate the volumetric concentration of FL molecules in the self-assembled films, assuming that the oscillator strength within the bilayers is similar to the one reported for the monomer in solution. Considering a molar absorption coefficient of 74 000 M^{-1} $cm^{-1} = 7.4 \times 10^7$ mol^{-1} cm^2 (18), and a bilayer absorbance of 0.0017 at the maximum (Figure 2a), it is possible to estimate a numeric density in the order of $0.0017 \times 6.02 \times 10^{23}/7.4 \times 10^7$ $cm^{-2} = 0.14$ molecules/nm^2. Considering a density of 3.7 positive charges nm^{-2} within the polyelectrolyte bilayer (17), it can be deduced that FL is incorporated at a ratio of one molecule every 27 PDDA monomeric units (P/D $\approx$ 27). Remaining polyelectrolyte charges are compensated by Cl^- or OH^- ions during assembly. Adding a new polyelectrolyte layer, dye molecules originally bound to the last one bind to the newly formed layer, shifting one counterion. Currently, the spectroscopic properties of the assemblies depend on the nature of the last layer, either dye or polyelectrolyte, because the dye arrangement is quite different in both situations (16). Assuming a bilayer thickness of 0.53 nm (16), a volumetric concentration of the dye in the order of 0.4 M is obtained. The dianionic dye is the predominant species within the bilayers, without any spectroscopically relevant degree of aggregation, despite its high local concentration.

A significant desorption of FL is observed in aqueous solution. Films formed with RB are comparatively more stable and allow the accumulation of subsequent bilayers without substantial loss of dye. Attempts to change the dye concentration in the films by varying the composition of the dipping solutions were unsuccessful. More concentrated solutions do not yield higher incorporation. This is understandable in RB films because the polyelectrolyte is nearly saturated with dye molecules. Even though the *P/D* ratio is much higher in the FL films, loading remains essentially unaffected on increasing the dye concentration. In the latter

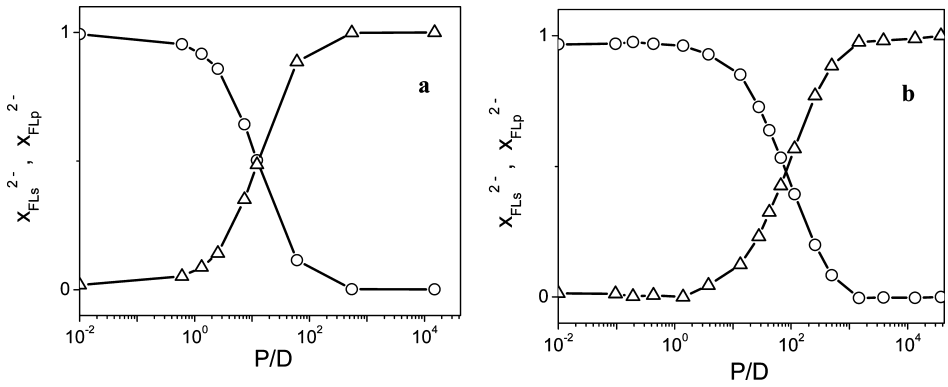

FIGURE 4. Speciation diagram of FL in PDDA solution as a function of the P/D ratio: monomer in solution (FL_s^{2-}, circles), and polyelectrolyte-associated monomers (FL_p^{2-}, triangles) at pH (a) ~10 and (b) ~12.

case, the dye is partially dissolved when the film is inmersed into the polyelectrolyte solution, especially at higher PDDA concentrations, pointing to an intrinsic instability of the assembly (13). Furthermore, at lower dye or polyelectrolyte concentrations, films do not grow. Therefore, very narrow concentration ranges are compatible with stable film formation. Although the charge of PDDA does not depend on the pH of the medium, the investigated xanthene dyes are protonated upon pH reduction, yielding monoanionic, neutral, and even monocationic species that are not suitable for self-assembly. On the other hand, hydroxyl ions inhibit FL incorporation, imposing an upper pH limit. Increasing the ionic strength with bases, acids, or salts induces coiling of the polyelectrolite in solution and in the film, rendering films with quite different properties (25).

Experiments in Solution. To gain further understanding on the self-assembly process, we carried out a systematic study in aqueous media by adding PDDA to a cell containing a solution of the dye, and measuring the absorption and fluorescence spectra for different P/D ratios. Experiments carried out by reversing the addition sequence, i. e., adding the dye to a solution of PDDA, reproduced the previously obtained results, thus revealing that the adsorption equilibrium is readily achieved.

In the case of RB, incorporation of the dye into the polyelectrolyte matrix occurs quantitatively at low PDDA concentrations building up aggregates up to P/D = 2. In this point, the charges of the dye and the polymer are fully compensated. Further addition of polyelectrolyte causes deaggregation of the dye, which remains associated with PDDA in the dianionic form. The incorporation and further deaggregation remain unaffected in a wide pH range, from 8 to 11 (17). Figure 3 summarizes the results of subsequent additions of PDDA to a 7.6×10^{-7} M aqueous RB solution. The molar fractions of each species were obtained by the analysis of the absorption and fluorescence spectra (for further details, see the Supporting Information).

The experiments carried out with FL in aqueous alkaline solution reveal a contrasting behavior, as compared with RB. As can be noticed from the speciation diagrams shown in Figure 4, at pH ~10 and ~12 an equilibrium between the dye in the aqueous phase and the PDDA matrix is established. The incorporation of FL sets in at higher P/D ratios than those found for RB and occurs in the monomeric dianionic form, without evidence of aggregation. The increase in pH has a negative effect upon incorporation, just as in film formation, revealing a competition between the anionic dye and the hydroxyl anions for the cationic adsorption sites in the polyelectrolyte.

The behavior of RB and FL is consistent with the difference in aggregation tendencies in solution. For RB, aggregation in water is mainly determined by hydrophobic interactions and the value of the dimerization constant is 250 M^{-1}. On the other hand, FL shows a 50 times smaller tendency toward dimer formation, which is otherwise predominantly related to hydrogen bonding (26). Charge compensation and free rotation of the monomers within the polyelectrolyte are factors that enhance hydrophobic interactions of RB in water solution, inducing dye aggregation and folding of the polyelectrolyte chain (17). In the case of FL, its displacement by hydroxyl anions evidences a weaker interaction with PDDA, which results in a less extended incorporation into the polyelectrolyte chain and incomplete charge compensation, hampering polyelectrolyte folding.

CONCLUSIONS

The unfolded conformation of PDDA within the bilayers (17) provides uniformly distributed charged sites for the adsorption of the dye. The resulting high degree of organization markedly reduces the formation of RB aggregates, which actually make up to 55% of the dye at an effective concentration near 1 M. At the same P/D ratio, aggregation is massive in solution. These characteristics of the material allow the emission of fluorescence (17) and $^1O_2$ generation owing to the presence of monomeric dye but do not entirely avoid energy trapping. FL-based films, on the other hand,

Scheme 1. Correlation among Structural and Physicochemical Properties

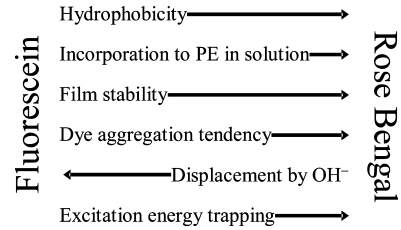

do not show aggregation at all but are rather prone to desorption of the dye, which is easily displaced by hydroxyl anions. The need to reach higher P/D ratios for the quantitative incorporation of the latter dye in solution is consistent with the higher lability of the corresponding arrays. Scheme 1 summarizes the correlations existing between the hydrophobicity of the dye, its aggregation tendency, and the properties associated with its incorporation into the polyelectrolyte in self-assembled arrays as well as in solution. The more hydrophobic RB displays an extended degree of aggregation if compared with FL, and consequently adds to the stabilization of the films. Therefore, a higher tendency toward dye aggregation results in greater film stability toward dye leakage but increases the probability of energy trapping.

Acknowledgment. Funding was obtained from CONICET (PIP 0319), ANPCyT (PICT 00938), and UBA (UBACyT X202). E.S.R. is a staff member of CONICET. M.M. acknowledges CONICET for a postgraduate fellowship. We are also grateful to Prof. L. De Cola, who kindly allowed the performance of IR phosphorescence measurements in her laboratory.

Supporting Information Available: Experimental details (PDF). This material is available free of charge via the Internet at http://pubs.acs.org.

REFERENCES AND NOTES

(1) Dai, Z.; Dähne, L.; Donath, E.; Möhwald, H. *J. Phys. Chem. B* **2002**, *106*, 11501–11508.
(2) van Laar, F. M. P. R.; Holsteyns, F.; Vankelecom, I. F. J.; Smeets, S.; Dehaen, W.; Jacobs, P. A. *J. Photochem. Photobiol. A: Chem.* **2001**, *144*, 141–151.
(3) Palmisano, G.; Gutiérrez, M. C.; Ferrer, M. L.; Gil-Luna, M. D.; Augugliaro, V.; Yurdakal, S.; Pagliaro, M. *J. Phys. Chem. C* **2008**, *112*, 2667–2670.
(4) DeRosa, M. C.; Crutchley, R. J. *Coord. Chem. Rev.* **2002**, *233–234*, 351–371.
(5) López, S. G.; Worringer, G.; Rodríguez, H. B.; San Román, E. *Phys. Chem. Chem. Phys.* **2010**, *12*, 2246–2253.
(6) Paczkowski, J.; Neckers, D. C. *Macromolecules* **1985**, *18*, 1245–1253.
(7) Rodríguez, H. B.; San Román, E. *Ann. N.Y. Acad. Sci.* **2008**, *1130*, 247–252.
(8) Iler, R. K. *J. Colloid Interface Sci.* **1966**, *21*, 569–594.
(9) Decher, G.; Schlenoff, J. B. *Multilayer Thin Films. Sequential Assembly of Nanocomposite Materials*; Wiley-VCH: Weinheim, Germany, 2003.
(10) Lvov, Y.; Decher, G.; Sukhorunov, G. *Macromolecules* **1993**, *26*, 5396–5399.
(11) Calvo, E. J.; Etchenique, R.; Pietrasanta, L.; Wolosiuk, A. *Anal. Chem.* **2001**, *73*, 1161–1168.
(12) Ariga, K.; Lvov, Y.; Kunitake, T. *J. Am. Chem. Soc.* **1997**, *119*, 2224–2231.
(13) Linford, M. R.; Auch, M.; Möhwald, H. *J. Am. Chem. Soc.* **1998**, *120*, 178–182.
(14) Lee, S.-H.; Kumar, J.; Tripathy, S. K. *Langmuir* **2000**, *16*, 10482–10489.
(15) Rousseau, E.; Koetse, M. M.; Van der Auweraer, M.; De Schryver, F. C. *Photochem. Photobiol. Sci.* **2002**, *1*, 395–406.
(16) Nicol, E.; Moussa, A.; Habib-Jiwan, J.-L.; Jonas, A. M. *J. Photochem. Photobiol. A: Chem.* **2004**, *167*, 31–35.
(17) Mirenda, M.; Dicelio, L. E.; San Román, E. *J. Phys. Chem. B* **2008**, *112*, 12201–12207.
(18) Sjöback, R.; Nygren, J.; Cubista, M. *Spectrochim. Acta, Part A* **1995**, *51*, L7–L21.
(19) Neckers, D. C. *J. Photochem. Photobiol. A: Chem.* **1989**, *47*, 1–29.
(20) Usui, Y. *Chem. Lett.* **1973**, *2*, 743–744.
(21) Braun, A. M.; Maurette, M.-T.; Oliveros, E. *Technologie Photochimique*; Presses Polytechniques Romandes: Lausanne, Switzerland, 1986.
(22) Wilkinson, F.; Helman, W. P.; Ross, A. B. *J. Phys. Chem. Ref. Data* **1993**, *22*, 113–262.
(23) Rohatgi, K. K.; Mukhopadhyay, A. K. *Photochem. Photobiol.* **1971**, *14*, 551–559.
(24) Lopez Arbeloa, I. *J. Chem. Soc., Faraday Trans.* **1981**, *2*, 1725–1733.
(25) McAloney, R. A.; Sinyor, M.; Dudnik, V.; Goh, M. C. *Langmuir* **2001**, *17*, 6655–6663.
(26) Valdes-Aguilera, O.; Neckers, D. C. *Acc. Chem. Res.* **1989**, *22*, 171–177.

AM100195V